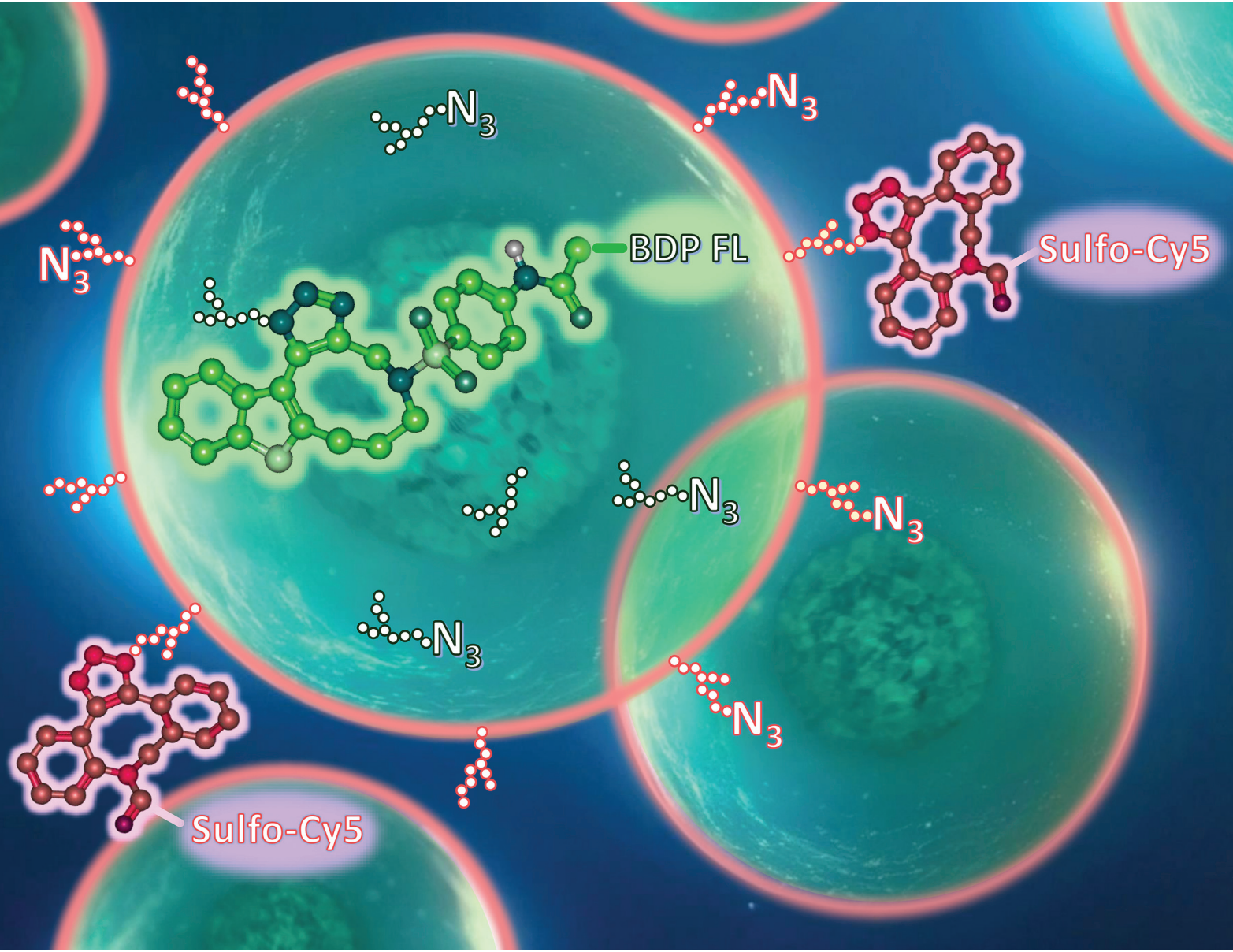


# Organic & Biomolecular Chemistry

rsc.li/obc



ISSN 1477-0520

**PAPER**

Stefan Bräse, Natalia A. Danilkina *et al.*

Key role of cycloalkyne nature in alkyne-dye reagents  
for enhanced specificity of intracellular imaging by  
bioorthogonal bioconjugation



Cite this: *Org. Biomol. Chem.*, 2024, 22, 7637

## Key role of cycloalkyne nature in alkyne-dye reagents for enhanced specificity of intracellular imaging by bioorthogonal bioconjugation†‡

Alexandra A. Vidyakina, <sup>a</sup> Sergey A. Silonov, <sup>a,b</sup> Anastasia I. Govdi, <sup>a</sup> Alexander Yu. Ivanov, <sup>c</sup> Ekaterina P. Podolskaya, <sup>d</sup> Irina A. Balova, <sup>a</sup> Stefan Bräse <sup>\*e,f</sup> and Natalia A. Danilkina <sup>\*a</sup>

Received 20th June 2024,  
Accepted 2nd July 2024

DOI: 10.1039/d4ob01032a  
rsc.li/obc

Conjugates of benzothiophene-fused azacyclononyne **BT9N-NH<sub>2</sub>** with fluorescent dyes were developed to visualise azidoglycans intracellularly. The significance of the cycloalkyne core was demonstrated by comparing new reagents with DBCO- and BCN-dye conjugates. To reduce non-specificity during intracellular bioconjugation using SPAAC, less reactive BT9N-dye reagents are preferred over highly reactive DBCO- and BCN-dye conjugates.

Bioorthogonal chemistry<sup>1</sup> is a modern field of research that aims to study complex biological systems using organic reactions, which do not interfere with biosystems and are not influenced by them.<sup>2,3</sup> These bioorthogonal click reactions have a wide range of applications.<sup>4–8</sup> Strain-promoted azide-alkyne cycloaddition (SPAAC) is one of the most widely used bioorthogonal transformations.<sup>9–12</sup> SPAAC has been used to study cell-surface glycosylation,<sup>13</sup> receptors engineering,<sup>14</sup> to design therapeutic proteins, *e.g.*, lysosome-targeting chimeras<sup>15</sup> and anticancer immunobiologics.<sup>16</sup> Nowadays, SPAAC is a common tool for visualising biomolecules,<sup>17–19</sup> such as proteins,<sup>20,21</sup> glycans,<sup>22,23</sup> and nucleic acids<sup>24</sup> through fluorescent labelling *in vitro* and *in vivo*.<sup>25</sup>

SPAAC visualisation typically involves two steps. The first step is aimed at incorporating azido groups into the biosystem either through metabolic labelling,<sup>26</sup> *i.e.*, cell culturing in the

presence of unnatural azido monomers, or using organic azides with “directing” groups for specific organelles, such as mitochondria, lysosomes, Golgi apparatus, without metabolic incorporation into biopolymers.<sup>27,28</sup> The second step involves the SPAAC reaction between the N<sub>3</sub>-containing cell compartments and a cycloalkyne reagent conjugated with a fluorescent dye.

Depending on the studied N<sub>3</sub>-labelled biological target, the cycloalkyne dye reagent should be able to reach the desired cell compartments. When labelling cell surface glycoproteins, it is important to use SPAAC active cycloalkyne reagents that cannot penetrate the cell membrane well to avoid nonspecific intracellular interactions. A dye with polar anionic groups, *e.g.*, from the sulfonyanine family, should be attached to the reactive cycloalkyne core to achieve this property.<sup>23,29</sup> To study intracellular N<sub>3</sub>-labelled biomolecules, the reagent must effectively penetrate the cell membrane.<sup>30,31</sup> To achieve this, a lipophilic dye component without any polar anionic groups, commonly different BODIPY derivatives, or other<sup>32</sup> should be conjugated with the alkyne. Therefore, nowadays, different companies offer several SPAAC reagents conjugated to dyes of different natures.

Although a wide variety of cycloalkynes with different SPAAC reactivity and other properties have been developed,<sup>33–36</sup> the cycloalkyne nature is often overlooked and not taken into account in the case of intracellular biovisualisation. The choice of alkyne moieties in the commercially available cycloalkyne-dye reagents is limited to the most commonly used commercial conjugates with highly SPAAC-reactive **DBCO** (**ADIBO**, **DIBAC**)<sup>37</sup> or **BCN**<sup>38</sup> cycloalkyne scaffolds (Fig. 1A), which were originally developed as cell-surface labelling reagents.

<sup>a</sup>Institute of Chemistry, Saint Petersburg State University (SPbU), Saint Petersburg, 199034, Russia. E-mail: n.danilkina@spbu.ru

<sup>b</sup>Laboratory of Structural Dynamics, Stability and Folding of Proteins, Institute of Cytology, Russian Academy of Sciences, 194064, Russia

<sup>c</sup>Center for Magnetic Resonance, Research Park, Saint Petersburg State University (SPbU), Saint Petersburg, 199034, Russia

<sup>d</sup>Institute of Analytical Instrumentation RAS, 190103 St. Petersburg, Russia

<sup>e</sup>Institute of Organic Chemistry (IOC), Karlsruhe Institute of Technology (KIT), 76131 Karlsruhe, Germany. E-mail: stefan.braese@kit.edu

<sup>f</sup>Institute of Biological and Chemical Systems – Functional Molecular Systems (IBCS-FMS), Karlsruhe Institute of Technology (KIT), 76344 Eggenstein-Leopoldshafen, Germany

† Dedicated to the 300th anniversary of the Saint Petersburg University foundation.

‡ Electronic supplementary information (ESI) available: All synthetic and biological details, copies of NMR spectra. See DOI: <https://doi.org/10.1039/d4ob01032a>



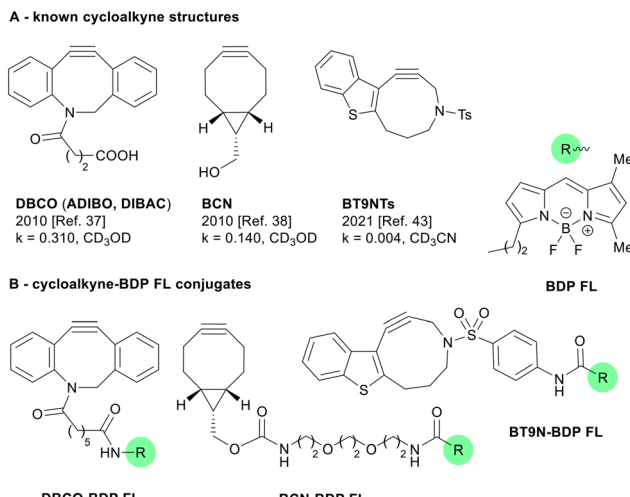


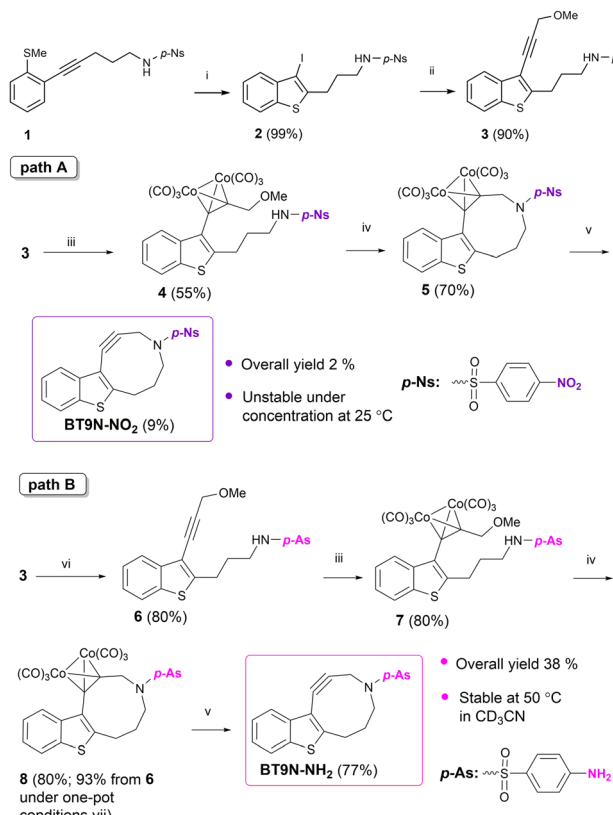
**Fig. 1** Structures of known DBCO- and BCN-based BDP FL reagents and new BT9N-BDP FL dye conjugates studied in this work;  $k$  – SPAAC reactivity constant for  $\text{BnN}_3, \text{M}^{-1} \text{s}^{-1}$ .

However, neglecting the cycloalkane nature, especially when intracellular staining of metabolically labelled compartments is involved, can lead to a high nonspecific fluorescence response due to the known reactivity of BCN and DBCO towards thiols (such as cysteine residues and glutathione)<sup>39</sup> and sulfenic acids,<sup>40–42</sup> which are common in biosystems.

Therefore, here we study the development of new reagents for efficient intracellular labelling, paying major attention to the cycloalkyne's nature. We synthesized a cycloalkyne-BODIPY-FL conjugate **BT9N-BDP FL** (Fig. 1B), an analogue of **BT9NTs**<sup>43</sup> (Fig. 1A), and compare its efficiency and specificity for the intracellular labelling with other BODIPY-FL cycloalkyne reagents having more reactive in SPAAC DBCO and BCN alkyne cores (Fig. 1B). We demonstrated that for the visualisation of intracellular  $\text{N}_3$ -glycoconjugates the nature of cycloalkyne is dramatically important. The designed **BT9N-BDP FL** reagent and its triazole-conjugated analogue **BT9N-Tr** have an advantage over **DBCO-BDP FL** and **BCN-BDP FL**, which showed significantly higher nonspecific affinity towards the intracellular environment.

The prototype of the **BT9N-BDP FL** conjugate is the **BT9NTs** cycloalkyne from heterocycle-fused heterocycloalkyne family (Fig. 1), which has been discovered recently<sup>43,44</sup> using a combination of the “reagent destabilisation” and the “SPAAC transition state stabilisation” approaches.<sup>11</sup> **BT9NTs** possess the highest SPAAC reactivity within this group, but it is unsuitable for conjugation with a dye because the molecule lacks any reactive functionalities. To synthesise the **BT9N-BDP FL** conjugate, we decide to replace the Ts group with 4-aminobenzenesulfonamide (As) moiety and use the  $\text{NH}_2$  group of **BT9N-NH<sub>2</sub>** as a site for functionalisation with a **BDP FL** dye.

The starting material chosen was 4-nitro-*N*-(pent-4-yn-1-yl)benzenesulfonamide (**S1**). The synthetic route for **BT9N-NH<sub>2</sub>** is similar to that for **BT9NTs**<sup>43</sup> and consists of three main



**Scheme 1** Optimisation of the synthetic procedure of **BT9N-NH<sub>2</sub>**. Reagents and conditions: (i)  $\text{I}_2$ , DCM, r.t., 1 h; (ii) methyl propargyl ether,  $\text{Pd}(\text{PPh}_3)_4$  (5.00 mol%),  $\text{CuI}$  (15.0 mol%),  $\text{KF}$ , DMF, 50 °C, 3 h; (iii)  $\text{Co}_2(\text{CO})_8$ , benzene,  $c = 0.01 \text{ M}$ , r.t., 2–3 h; (iv)  $\text{BF}_3\text{-OEt}_2$ , DCM,  $c = 0.001 \text{ M}$ , 0 °C to r.t., 2 h; (v)  $\text{TBAF-H}_2\text{O}$  acetone/ $\text{H}_2\text{O}$  (15:1),  $c = 0.006 \text{ M}$ , r.t., 4–5 h; (vi) Fe powder,  $\text{NH}_4\text{Cl}$ , acetone/ $\text{H}_2\text{O}$  (1:1), 40 °C, 48 h; (vii) Co-complexation/Nicholas reaction in one-pot:  $\text{Co}_2(\text{CO})_8$  DCM = 0.01 M, r.t., 2 h, then  $\text{BF}_3\text{-OEt}_2$ , DCM,  $c = 0.0035 \text{ M}$ , 0 °C to r.t., 15 min.

steps: the Sonogashira cross-coupling, electrophile-promoted cyclisation and the Nicholas cyclisation (Scheme 1). The main question was at what stage the nitro group should be reduced. First, we decided to reduce  $\text{NO}_2$  at the last stage under conditions that tolerated up to a triple bond<sup>45</sup> and obtain the nitroalkyne **BT9N-NO<sub>2</sub>** via pathway A (Scheme 1, path A). However, due to its instability, the cycloalkyne **BT9N-NO<sub>2</sub>** without the Co-protecting group was only isolated in a 9% yield. To overcome this problem, we moved the  $\text{NO}_2$  reduction step to an earlier stage and tried the Nicholas cyclisation for the  $\text{NH}_2$  derivative **7** (Scheme 1, path B). Although the Nicholas reaction for  $\text{NH}_2$ -containing compounds does not go well,<sup>46</sup> to our delight, this reaction for the amino Co-complex **7** gave the desired cyclic product **8** in high yield without forming any by-products. Complex **8** can be obtained even in higher yield using Co-complexation/Nicholas cyclisation in one pot. Cycloalkyne **BT9N-NH<sub>2</sub>** obtained by deprotection of complex **8** showed excellent stability under isolation, storage and heating at 50 °C for 24 hours in  $\text{CD}_3\text{CN}$ .



We then turned to the synthesis of the **BT9N-BDP FL** conjugate. However, 4-aminobenzenesulfonamide moiety was inert towards electrophilic agents, *e.g.* isothiocyanates, anhydrides and carboxylic acids with coupling reagents (ESI, section 2.3‡). Finally, we found that **BT9N-NH<sub>2</sub>** could be modified by acylation with acetyl chloride (ESI, 2.3.2‡). Therefore, BDP FL acid chloride<sup>47</sup> was used to synthesise **BT9N-BDP FL** under optimised conditions (Scheme 2) (ESI, section 2.2‡).

The synthesis of another example of the **BT9N** SPAAC reagent, **BT9N-Tr** (Scheme 2), followed the same procedure. This reagent was examined as an additional **BT9N**-dye conjugate with a non-commercial lipophilic dye belonging to a pull-push triazole family.<sup>48</sup> This would demonstrate the importance of the cycloalkyne nature for intracellular biovisualisation, irrespective of a lipophilic dye core. **BCN-BDP FL** was synthesised using commercially available **BCN-NH<sub>2</sub>** and **BDP FL** NHS ester (ESI, section 2.2‡). The **DBCO-BDP FL** conjugate was obtained from Lumiprobe, a commercial supplier.

Using four different cycloalkyne reagents (**BT9N-BDP FL**, **BT9N-Tr**, **BCN-BDP FL** and **DBCO-BDP FL**), we performed biological studies to demonstrate the importance of the cycloalkyne core in the intracellular visualisation of metabolically labelled azido glycans. Before the studies, the cytotoxicity of all compounds was evaluated using HeLa and HEK293 cell lines (ESI, Fig. S1‡). All reagents were nontoxic under concentration of 1  $\mu$ M, which was used for all further bioimaging assays.

Three different azidosugars were studied: **Ac<sub>4</sub>ManNAz** (tetraacetylated *N*-azidoacetyl-mannosamine) was used as a sugar known to be the component of sialic acid found on the cell surface, **Ac<sub>4</sub>GalNAz** (tetraacetylated *N*-azidoacetyl-galactosamine) was used a source of mucin O-linked glycosylation for both cell surface and intracellular glycans and **Ac<sub>4</sub>GlcNAz** (tetraacetylated *N*-azidoacetyl-glucosamine) was used for mostly intracellular labelling.<sup>13,27,49</sup>

HeLa cells were treated with the corresponding acylated  $N_3$ -sugar for 72 hours. Subsequently, they were stained with the corresponding cycloalkyne-dye conjugate for 4 hours (Fig. 2A). To control the distribution of each azidosugar on the cell surface, two **DBCO** reagents were used: one conjugated with fluorescein dye (**DBCO-F**) and the other with Sulfocyanine 5 dye (**DBCO-SCy5**) (Fig. 2B and C).

The data obtained revealed that both **BT9N**-dye conjugates, **BT9N-BDP FL** and **BT9N-Tr**, demonstrate significantly higher specificity in  $N_3$ -dependent intracellular labelling of

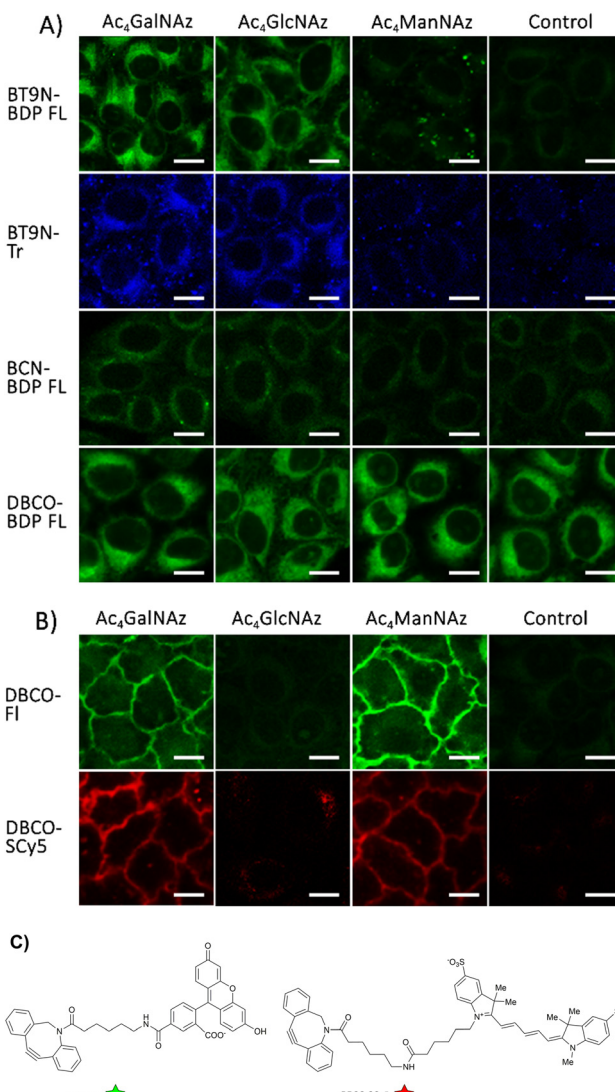
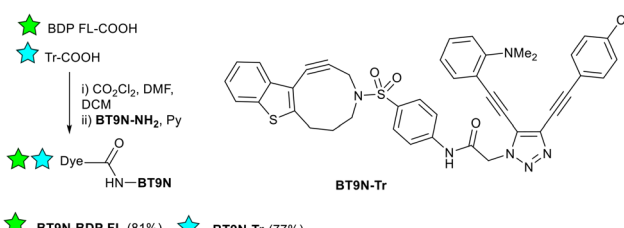


Fig. 2 Confocal fluorescent imaging of HeLa cells treated with the corresponding sugars (50  $\mu$ M, 72 h) and then incubated with the respective alkyne-dye conjugate (1  $\mu$ M, 4 h) **BT9N-BDP FL**, **BT9N-Tr**, **BCN-BDP FL**, **DBCO-BDP FL** (A) and **DBCO-FL**, **DBCO-SCy5** (B); structures of **DBCO-FL** and **DBCO-SCy5** are represented in (C). Fluorescence images for **BT9N-BDP FL**, **BCN-BDP FL**, **DBCO-BDP FL**, and **DBCO-FL** conjugates were captured using the FITC channel (Ex. 488 nm, Em. 500–550 nm); for **BT9N-Tr**, the DAPI channel was used (Ex. 406 nm, Em. 425–475 nm); for **DBCO-SCy5**, the Cy5 channel was used (Ex. 638 nm, Em. 663–738 nm)—scale bar: 15  $\mu$ m.



Scheme 2 Synthesis of **BT9N**-Dye conjugates.

**Ac<sub>4</sub>GalNAz** and **Ac<sub>4</sub>GlcNAz** treated cells compared to **BCN-BDP FL** and **DBCO-BDP FL**. These two latter conjugates displayed serious nonspecific labelling in non-treated control cells (for a quantitative comparison of the fluorescent response, refer to the ESI, Fig. S2‡). Furthermore, only weak fluorescence was observed in **Ac<sub>4</sub>ManNAz** metabolically labelled cells for both **BT9N** conjugates, which confirms the known cell-surface localisation of the deacylated mannosamine. The significantly stronger intracellular fluorescence observed in **Ac<sub>4</sub>ManNAz** treated cells for **BCN-BDP FL** and **DBCO-BDP FL** is likely due



to the nonspecific binding of alkyne-dye conjugates with the intracellular environment.

It is interesting to note that **DBCO-BDP FL** exhibited greater nonspecific intracellular labelling compared to **BCN-BDP FL**, which is consistent with the general reactivity of **DBCO**.<sup>37,50</sup>

The nonspecific behaviour of **DBCO** and **BCN** reagents in cells is more likely due to their high reactivity not only in SPAAC but also with other “alkynophiles” present in the biological environment, such as the -SH and -SOH groups of proteins.

Thus it has been shown, that **BCN** and **DBCO** can react with peptidylcysteines, which is the reason of azide-independent labeling and that it can be diminished by iodoacetamide alkylation of thiols.<sup>39</sup> Moreover the reactivity of **BCN** and **DBCO** towards sulfenic acids has been also proved.<sup>40–42</sup>

We have recently reported that the prototype of **BT9N**-based dyes, a cycloalkyne **BT9NTs**, does not react with *t*-BuSH in  $\text{CD}_3\text{CN}$  even at 37 °C for 24 h.<sup>43</sup> To demonstrate that cycloalkyne-dye reagents **BT9N-BDP FL** and **BT9N-Tr** are less reactive than **DBCO** and **BCN** dyes towards SH-containing biospecies, we conducted a study investigating the behavior of all four compounds towards glutathione (GSH) and human globin using MALDI TOF mass spectrometry (for details see ESI, section 5‡).<sup>51</sup> It was estimated that **DBCO** and **BCN** dyes form adducts with human globin (alpha and beta subunits) after 3 hours of incubation at 37 °C (pH = 7.2), while **BT9N**-dyes do not react with the protein. Furthermore, we identified mono- and bis-adducts of **DBCO** and a monoadduct of **BCN** with GSH using 2,5-dihydroxybenzoic acid (DHB) and  $\alpha$ -cyano-4-hydroxycinnamic acid (CHCA) as a matrix for MALDI spectra. In the case of **BT9N-BDP FL**, only a monoadduct was identified using the DHB matrix, whereas no adducts were observed for **BT9N-Tr** in both matrices. Therefore, our findings indicate that less SPAAC reactive cycloalkyne-dye conjugates, based on **BT9N**, display increased tolerance towards endogenous thiol species in comparison with more active **DBCO** and **BCN** derivatives.

To demonstrate the pivotal role of selecting of the optimal cycloalkyne as a component of a cycloalkyne-dye reagent in achieving the desired outcomes of a study, we conducted double labelling experiments (Fig. 3).

In order to label intracellular and cell surface glycans in a single metabolic labelling experiment, either  $\text{Ac}_4\text{GalNAz}$  or both  $\text{Ac}_4\text{ManNAz}$  and  $\text{Ac}_4\text{GlcNAz}$  were employed in the metabolic labelling of HeLa (Fig. 3A) and HEK293 (Fig. 3B) cell lines. **BT9N-BDP FL** and **DBCO-SCy5** were used in order to simultaneously visualise intracellular and surface  $\text{N}_3$ -glycans in green and red channels, respectively. The merged images for both cell lines in every case demonstrated that **BT9N-BDP FL** is an effective reagent for visualising intracellular azidoglycans ( $\text{N}_3$ -glucose and intracellular  $\text{N}_3$ -galactose), while **DBCO-SCy5** is a reagent of choice for visualising cell surface glycans ( $\text{N}_3$ -mannose and cell surface  $\text{N}_3$ -galactose). It is of paramount importance that both reagents act orthogonally and can be employed for the labelling of corresponding glycans during a single double-labelling experiment.

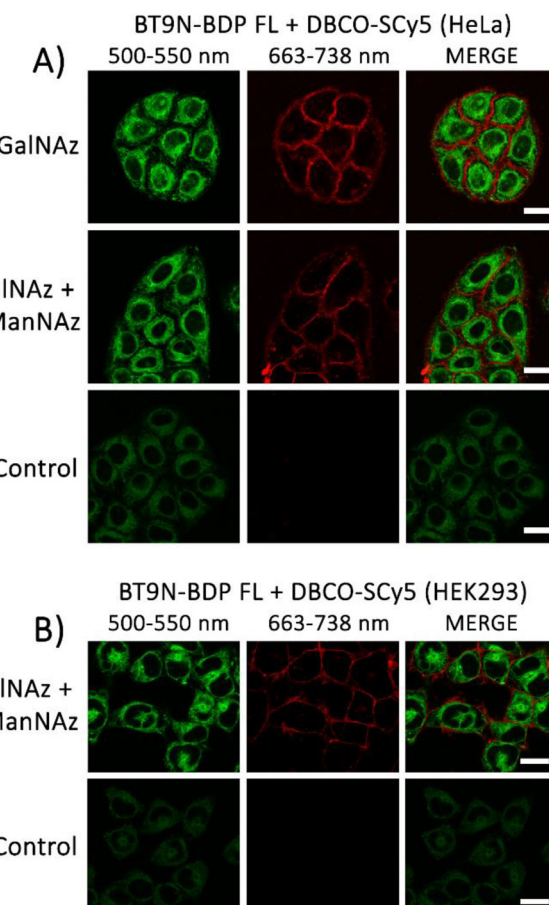


Fig. 3 Confocal fluorescent imaging of HeLa (A) and Hek293 (B) cells treated with the corresponding sugars (50  $\mu\text{M}$ , 72 h) and then incubated first with **BT9N-BDP FL** (1  $\mu\text{M}$ , 3 h), and then with **DBCO-SCy5** (1  $\mu\text{M}$ , 30 min) for double intracellular and cell surface labelling, respectively. Fluorescence images for **BT9N-BDP FL** conjugates were captured using the FITC channel (Ex. 488 nm, Em. 500–550 nm); for **DBCO-SCy5**, the Cy5 channel was used (Ex. 638 nm, Em. 663–738 nm)—scale bar: 20  $\mu\text{m}$ .

## Conclusions

Azacyclononyne dye conjugates **BT9N-BDP FL**, and **BT9N-Tr** have been developed for intracellular fluorescent labelling of  $\text{N}_3$ -glycans containing cells. We have demonstrated the important role of the cycloalkyne core for intracellular bioimaging. Even though **BT9N** derivatives have significantly slower SPAAC kinetics with azides compared to the two well-known cyclooctynes (**BCN** and **DBCO**), we have shown that in the case of intracellular biorthogonal bioconjugation, this disadvantage turns into an advantage due to minimal nonspecific binding of **BT9N** derivatives with the intracellular bioenvironment.

## Author contributions

AAV and SAS contributed equally to this work. AAV – investigation, methodology, writing – original draft; SAS – investi-



gation, methodology, visualisation; AIG – investigation; AYU1 – formal analysis; EPP – investigation; IAB – project administration, supervision; SB – project administration, supervision, writing – review & editing; NAD – conceptualization, data curation, methodology, project administration, supervision, visualization, funding acquisition, writing – original draft, writing – review & editing.

## Data availability

The data supporting this article have been included as part of the ESI‡: synthetic procedures, MTT test details, cell culture and confocal microscopy, MALDI TOF mass spectrometry details and copies of MS spectra, copies of NMR spectra of all synthesized compounds.

## Conflicts of interest

There are no conflicts to declare.

## Acknowledgements

This work was funded by the Russian Science Foundation 24-23-00377. The research was carried out using the SPbU Resource Centres: Magnetic Resonance Research Centre, Chemical Analysis and Materials Research Centre, Centre for Optical and Laser Materials Research, Center for Molecular and Cell Technologies; Oussama Abdelhamid Mammeri (SPbU) is thanked for ESI HR MS measurements.

## References

- 1 J. A. Prescher and C. R. Bertozzi, *Nat. Chem. Biol.*, 2005, **1**, 13–21.
- 2 T. Deb, J. Tu and R. M. Franzini, *Chem. Rev.*, 2021, **121**, 6850–6914.
- 3 S. S. Nguyen and J. A. Prescher, *Nat. Rev. Chem.*, 2020, **4**, 476–489.
- 4 C. Pan, X. Jiang, C. Liu, J. Wei, Y. Wang, C. Yang and Y. Gan, *Chem. Eng. J.*, 2024, **480**, 148120.
- 5 R. E. Bird, S. A. Lemmel, X. Yu and Q. A. Zhou, *Bioconjugate Chem.*, 2021, **32**, 2457–2479.
- 6 Q. Zhang, G. Kuang, L. Wang, P. Duan, W. Sun and F. Ye, *Research*, 2023, **6**, 1–26.
- 7 E. Kim and H. Koo, *Chem. Sci.*, 2019, **10**, 7835–7851.
- 8 W. Yi, P. Xiao, X. Liu, Z. Zhao, X. Sun, J. Wang, L. Zhou, G. Wang, H. Cao, D. Wang and Y. Li, *Signal Transduction Targeted Ther.*, 2022, **7**, 386.
- 9 N. J. Agard, J. A. Prescher and C. R. Bertozzi, *J. Am. Chem. Soc.*, 2004, **126**, 15046–15047.
- 10 E. G. Chupakhin and M. Y. Krasavin, *Chem. Heterocycl. Compd.*, 2018, **54**, 483–501.
- 11 T. Harris and I. V. Alabugin, *Mendeleev Commun.*, 2019, **29**, 237–248.
- 12 J. Dommerholt, F. P. J. T. Rutjes and F. L. van Delft, *Top. Curr. Chem.*, 2016, **374**, 16.
- 13 H. Xiao, G. X. Tang and R. Wu, *Anal. Chem.*, 2016, **88**, 3324–3332.
- 14 C.-H. Lee, S. Park, S. Kim, J. Y. Hyun, H. S. Lee and I. Shin, *Chem. Sci.*, 2024, **15**, 555–565.
- 15 S. M. Banik, K. Pedram, S. Wisnovsky, G. Ahn, N. M. Riley and C. R. Bertozzi, *Nature*, 2020, **584**, 291–297.
- 16 P. A. Szijj, M. A. Gray, M. K. Ribi, C. Bahou, J. C. F. Nogueira, C. R. Bertozzi and V. Chudasama, *Nat. Chem.*, 2023, **15**, 1636–1647.
- 17 E. Kozma and P. Kele, *Top. Curr. Chem.*, 2024, **382**, 7.
- 18 G. B. Cserép, A. Herner and P. Kele, *Methods Appl. Fluoresc.*, 2015, **3**, 042001.
- 19 S. H. Alamudi, X. Liu and Y.-T. Chang, *Biophys. Rev.*, 2021, **2**, 021301.
- 20 S. H. Alamudi, R. Satapathy, J. Kim, D. Su, H. Ren, R. Das, L. Hu, E. Alvarado-Martínez, J. Y. Lee, C. Hoppmann, E. Peña-Cabrera, H.-H. Ha, H.-S. Park, L. Wang and Y.-T. Chang, *Nat. Commun.*, 2016, **7**, 11964.
- 21 P. Mateos-Gil, S. Letschert, S. Doose and M. Sauer, *Front. Cell Dev. Biol.*, 2016, **4**, 1–16.
- 22 X. Wen, B. Yuan, J. Zhang, X. Meng, Q. Guo, L. Li, Z. Li, H. Jiang and K. Wang, *Chem. Commun.*, 2019, **55**, 6114–6117.
- 23 S. K. Leong, Y. Chen, J. Hsiao, C. Tsai and J. Shie, *ChemBioChem*, 2023, **24**, 1–7.
- 24 J. Zayas, M. Annoual, J. K. Das, Q. Felty, W. G. Gonzalez, J. Miksovská, N. Sharifai, A. Chiba and S. F. Wnuk, *Bioconjugate Chem.*, 2015, **26**, 1519–1532.
- 25 D. Chen, Y. Lin, A. Li, X. Luo, C. Yang, J. Gao and H. Lin, *Anal. Chem.*, 2022, **94**, 16614–16621.
- 26 K. Dammen-Brower, E. Tan, R. T. Almaraz, J. Du and K. J. Yarema, *Curr. Protoc.*, 2023, **3**, e822.
- 27 S. H. Alamudi, D. Su, K. J. Lee, J. Y. Lee, J. L. Belmonte-Vázquez, H.-S. Park, E. Peña-Cabrera and Y.-T. Chang, *Chem. Sci.*, 2018, **9**, 2376–2383.
- 28 M. Xiao, Y. Zhang, R. Li, S. Li, D. Wang and P. An, *Chem. – Asian J.*, 2022, **17**, e202200634.
- 29 H. Stöckmann, A. A. Neves, S. Stairs, H. Ireland-Zecchini, K. M. Brindle and F. J. Leeper, *Chem. Sci.*, 2011, **2**, 932.
- 30 V. Šlachtová, M. Chovanec, M. Rahm and M. Vrabel, *Top. Curr. Chem.*, 2024, **382**, 2.
- 31 V. Rigolot, C. Biot and C. Lion, *Angew. Chem., Int. Ed.*, 2021, **60**, 23084–23105.
- 32 S. H. Alamudi and Y.-T. Chang, *Chem. Commun.*, 2018, **54**, 13641–13653.
- 33 Y. Hu, R. Spiegelhoff, K. S. Lee, K. M. Sanders and J. M. Schomaker, *J. Org. Chem.*, 2024, **89**, 4512–4522.
- 34 E. Das, M. A. M. Feliciano, P. Yamanushkin, X. Lin and B. Gold, *Org. Biomol. Chem.*, 2023, **21**, 8857–8862.
- 35 M. J. Holzmann, N. Khanal, P. Yamanushkin and B. Gold, *Org. Lett.*, 2023, **25**, 309–313.



- 36 J. Weterings, C. J. F. Rijcken, H. Veldhuis, T. Meulemans, D. Hadavi, M. Timmers, M. Honing, H. Ippel and R. M. J. Liskamp, *Chem. Sci.*, 2020, **11**, 9011–9016.
- 37 M. F. Debets, S. S. van Berkel, S. Schoffelen, F. P. J. T. Rutjes, J. C. M. van Hest and F. L. van Delft, *Chem. Commun.*, 2010, **46**, 97–99.
- 38 J. Dommerholt, S. Schmidt, R. Temming, L. J. A. Hendriks, F. P. J. T. Rutjes, J. C. M. van Hest, D. J. Lefeber, P. Friedl and F. L. van Delft, *Angew. Chem., Int. Ed.*, 2010, **49**, 9422–9425.
- 39 R. van Geel, G. J. M. Pruijn, F. L. van Delft and W. C. Boelens, *Bioconjugate Chem.*, 2012, **23**, 392–398.
- 40 T. H. Poole, J. A. Reisz, W. Zhao, L. B. Poole, C. M. Furdui and S. B. King, *J. Am. Chem. Soc.*, 2014, **136**, 6167–6170.
- 41 Z. Li, T. E. Forshaw, R. J. Holmila, S. A. Vance, H. Wu, L. B. Poole, C. M. Furdui and S. B. King, *Chem. Res. Toxicol.*, 2019, **32**, 526–534.
- 42 D. J. McGarry, M. M. Shchepinova, S. Lilla, R. C. Hartley and M. F. Olson, *ACS Chem. Biol.*, 2016, **11**, 3300–3304.
- 43 N. A. Danilkina, A. I. Govdi, A. F. Khlebnikov, A. O. Tikhomirov, V. V. Sharoyko, A. A. Shtyrov, M. N. Ryazantsev, S. Bräse and I. A. Balova, *J. Am. Chem. Soc.*, 2021, **143**, 16519–16537.
- 44 A. A. Vidyakina, A. A. Shtyrov, M. N. Ryazantsev, A. F. Khlebnikov, I. E. Kolesnikov, V. V. Sharoyko, D. V. Spiridonova, I. A. Balova, S. Bräse and N. A. Danilkina, *Chem. – Eur. J.*, 2023, **29**, e202300540.
- 45 K. Kaneda, R. Naruse and S. Yamamoto, *Org. Lett.*, 2017, **19**, 1096–1099.
- 46 N. A. Danilkina, E. A. Khmelevskaya, A. G. Lyapunova, A. S. D'Yachenko, A. S. Bunev, R. E. Gasanov, M. A. Gureev and I. A. Balova, *Molecules*, 2022, **27**, 6071.
- 47 B. Brandes, S. Hoenke, L. Fischer and R. Csuk, *Eur. J. Med. Chem.*, 2020, **185**, 111858.
- 48 A. I. Govdi, P. V. Tokareva, A. M. Rumyantsev, M. S. Panov, J. Stellmacher, U. Alexiev, N. A. Danilkina and I. A. Balova, *Molecules*, 2022, **27**, 3191.
- 49 N. J. Pedowitz and M. R. Pratt, *RSC Chem. Biol.*, 2021, **2**, 306–321.
- 50 C. Zhang, P. Dai, A. A. Vinogradov, Z. P. Gates and B. L. Pentelute, *Angew. Chem., Int. Ed.*, 2018, **57**, 6459–6463.
- 51 A. Gorbunov, A. Bardin, S. Ilyushonok, J. Kovach, A. Petrenko, N. Sukhodolov, K. Krasnov, N. Krasnov, I. Zorin, A. Obornev, V. Babakov, A. Radilov and E. Podolskaya, *Microchem. J.*, 2022, **178**, 107362.

